MINIMISING SYSTEMATIC ERROR SURFACES IN DIGITAL ELEVATION MODELS USING OBLIQUE CONVERGENT IMAGERY

Rene Wackrow (r.wackrow@lboro.ac.uk),
Jim H. Chandler (j.h.chandler@lboro.ac.uk),
Loughborough University

Abstract

There are increasing opportunities to use consumer grade digital cameras, particularly if accurate spatial data can be captured. Research recently conducted at Loughborough University, identified residual systematic error surfaces or domes, discernable in digital elevation models (DEMs). These systematic effects are often associated with such cameras and caused by slightly inaccurate estimated lens distortion parameters. Additionally, a methodology that minimises the systematic error surfaces was developed, which uses a mildly convergent image configuration in a vertical perspective (Wackrow and Chandler, 2008). This methodology was tested through simulation and a series of practical tests. This paper investigates the potential of the convergent configuration to minimise the error surfaces, even if the geometrically more complex oblique perspective is used. Initially, simulated data are used to demonstrate that an oblique convergent image configuration can minimise remaining systematic error surfaces using various imaging angles. Additionally, practical tests using a laboratory testfield were conducted to verify results of the simulation. The need to develop a system to measure the topographic surface of a flooding river provided the opportunity to verify the findings of the simulation and laboratory test using real data. Results of the simulation process, laboratory test and the practical test are reported in this paper and demonstrate that an oblique convergent image configuration eradicates the systematic error surfaces due to inaccurate lens distortion parameters. This approach is significant because by removing the need for an accurate lens model it effectively improves the accuracies of digital surface representations derived using consumer-grade digital cameras. Carefully selected image configurations could therefore provide new opportunities for improving the quality of photogrammetrically acquired data.

KEYWORDS: convergent image configuration, digital camera, close range photogrammetry, spatial measurement, digital elevation model

<center>INTRODUCTION</center>

Deriving accurate spatial data from a series of non-metric images is particularly important since consumer-grade digital cameras are becoming increasingly used for various spatial measurement applications. This includes areas ranging from: water engineering, heritage documentation and the earth sciences e.g. (Chandler et al., 2008; Remondino and Menna, 2008; Robson et al., 2008; Remondino et al., 2010). However, remaining systematic error surfaces or domes, discernable in digital elevation models (DEMs) of difference have been identified in past research (Hothmer, 1958, 1959; Fryer and Mitchell, 1987; Stojic et al., 1998; Chandler et al., 2003, 2005; Wackrow et al., 2007; Wackrow and Chandler, 2008). These remaining systematic effects can degrade accuracy in the object space, achievable with non-metric digital cameras.

The quality of derived spatial data can be defined as a function of precision, accuracy and reliability with respect to random, systematic and gross errors respectively (Cooper and Cross, 1988). The accuracy of data is the most significant for most users and is closely related to the eradication of systematic effects, but these are more difficult to detect and eradicate than random and gross errors. Calibrating instruments, for example consumer-grade digital cameras, can assist in minimising systematic effects, but accounting explicitly for all can be difficult because of high correlation between calibration parameters (Granshaw, 1980; Fraser, 1997; Maas, 1999). These difficulties justify seeking an alternative approach to minimise such systematic effects.

The use and importance of highly convergent image configuration networks is frequently reported in the literature but normally for camera calibration (e.g. Fraser, 2006; Remondino and Fraser, 2006). The use of convergent imagery for routine measurement such as DEM extraction is less frequently described. Accuracies in object-space coordinates for four non-metric cameras and a metric camera using convergent imagery were investigated by Karara and Abdel-Aziz (1974). Somewhat surprisingly, Karara and Abdel-Aziz (1974) concluded that the normal case is the most desirable configuration or the convergent angle should be kept as small as possible. In the field of medical science, Grenness et al. (2005) described an approach using convergent stereopairs and a semi-metric camera for modelling tooth replicas. An association between increasing the convergence angle of stereo-pairs and increasing precision is not suggested by Grenness et al. (2005). However, research recently conducted at Loughborough University demonstrated that using mildly vertical convergent imagery for DEM generation, minimises remaining systematic error surfaces or domes caused by slightly inaccurately estimated lens distortion parameters (Wackrow and Chandler, 2008). In a series of tests this study demonstrated that adopting such a configuration, provides an effective way of improving the accuracy achievable with consumer-grade digital cameras.

The purpose of this paper is to investigate whether similar benefits arise if an oblique configuration has to be adopted. This can increase the flexibility of the methodology described in Wackrow and Chandler (2008) since oblique image configurations are often desirable in close range photogrammetry applications. The methodology, developed to measure a dynamic water surface using an oblique

convergent image configuration is introduced (Wackrow et al., 2008), followed by simulated and experimental results. The paper then concludes with a discussion and brief summary.

MEASURING A DYNAMIC WATER SURFACE USING OBLIQUE CONVERGENT IMAGE PAIRS

In Wackrow and Chandler (2008), only vertical imagery and comparatively flat test objects had been used for simulations and practical tests. This was to investigate the potential of a convergent image configuration to minimise systematic error surfaces in DEMs created by an inaccurate lens model. A small river, situated in Loughborough, was selected as a study site to support the development of a technique to measure the topographic surface of a flooding river in Farnham, Surrey (Chandler et al., 2008). Visiting the study site at the river in Loughborough revealed that oblique image pairs would have to be used to measure the water surface. This provided the necessity and perhaps the opportunity to investigate whether a convergent image configuration can minimise the domes arising from an inaccurate lens model, even if the geometrically more complex oblique perspective is adopted.

Simulating an oblique image configuration

The systematic error surfaces created by an inaccurate lens model were investigated in Wackrow and Chandler (2008) using simulated data. This simulation process has proven to be an alternative and more productive approach to the use of real data because it overcomes the variability and uncertainties associated with conducting field work. The simulation allows full independent manipulation of parameters allowing true controls to be identified.

The flat and planar virtual testfield (Wackrow and Chandler, 2008) was used again to provide evenly distributed X, Y, Z coordinates of hundreds of object points representing the true geometry of the testfield. A set of predefined interior and two sets of exterior orientation parameters describing an image pair were used in the simulation. This represents either an oblique normal or oblique convergent image configuration (Figure 1) and perfect photo coordinates for the X, Y, Z coordinates of the virtual testfield were computed. Various image configurations with an imaging angle between 60 and 20 degrees were tested. Such configurations also create a significant depth in the object, contrary to the vertical image configurations tested in Wackrow and Chandler (2008). The parameter K_1 describing the radial lens distortion was changed by 20% to illustrate the effect of a significantly inaccurate lens model and to demonstrate forcibly the capability of the oblique convergent configuration to compensate for these effects. Although selection of a 20% change was arbitrary, a change of such magnitude could be envisaged if the zoom setting was inadvertently changed. It was also a value which would allow clear indication of the impact of such a systematic error. The other interior orientation parameters remained unmodified. The derived photo coordinates, the modified interior orientation and the exterior orientation were then re-established using the external bundle adjustment GAP (Chandler and

Clark, 1992) to compute object coordinates. These derived object coordinates therefore reflect the impact of changing the radial distortion parameter K_1 and were compared with the true geometry of the virtual testfield using a MATLAB routine. The results derived from this simulation are presented in the Results and Discussion section entitled "Simulation".
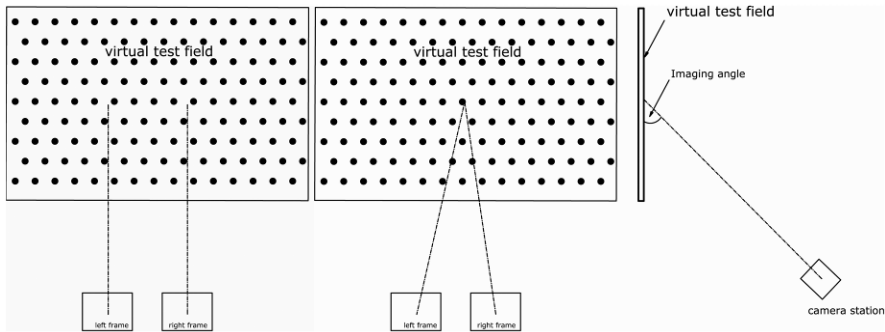

Figure 1. Camera configurations - oblique normal and convergent case

Practical test using a laboratory testfield

A 3D laboratory testfield was used to verify the results of the simulation process which was introduced in the previous section. The testfield was initially constructed for camera calibration purposes at close range. However, this test object provides also the opportunity to derive thousands of independent check points to allow the accuracy in the object space to be determined with sufficient statistical reliability (Chandler et al. 2005; Wackrow et al. 2007; Wackrow and Chandler 2008; Wackrow 2008). The testfield consists of a medium density fibreboard with added square blocks of various shape and heights. Additionally, 28 photogrammetric target points coordinated to sub-millimetre accuracy using theodolite intersection were used for image restitution and also used to create a digital elevation model (DEM) at 1mm resolution which represents the true geometry and shape of the test object, known as the "Truth DEM". The "Truth DEM" could be compared with automatically extracted DEM's by subtraction and interpolation which provided elevation differences for thousands of points. Using these elevation differences, mean error and standard deviation of error of DEM's of differences can be extracted and the achieved accuracy in the object space could be quantified. Results of these practical tests are presented in the Result and Discussion section entitled "Laboratory testfield".

Practical test measuring a dynamic water surface

A small river situated in Loughborough was used to conduct a simple and direct practical test to measure a dynamic water surface using a photogrammetric approach. The river was approximately 4 m wide and 0.3 to 0.4 m in depth under normal fluvial conditions. Temporary photogrammetric target points were

distributed along the river banks to provide conventional photogrammetric control (Figure 2). These were coordinated using a reflectorless Total Station (Leica TCR 1203).

Figure 2. Target point setup on the river in Loughborough

Evaluating the accuracy of derived data representing a dynamic water surface was identified as a particular challenge. Analysis of the residuals of the control points can be used as a first indication of accuracy of the network restitution, but is not independent because these points were used to compute the solution of the network. The dynamic nature of the water surface prevented the use of DEM of differences, which had been successfully employed to assess accuracy in the object space prior (Chandler et al., 2005; Wackrow et al., 2007; Wackrow and Chandler, 2008). However, using independent check point data was considered to be essential. Unfortunately, it was difficult to distribute a suitable number of check points close to the water surface of the running river. The solution adopted in this case involved placing a survey staff close to the water surface and using its graduations to provide appropriate check point data (Figure 3). The staff graduations were coordinated using the reflectorless Total Station and could be compared with estimates established by photogrammetry using both the normal and convergent image configurations. The accuracies achieved in the object space area in which the survey staff was positioned could be then quantified by analysing these data.

A bridge across the river provided an ideal platform to position a pair of Nikon D80 digital cameras (10 Mega-pixel), both equipped as standard with a variable zoom lens (AF-SDX Zoom-Nikkor 18-70 mm). The cameras were mounted on standard photographic tripods (Figure 5). Tests reported in Chandler et al. (2008) demonstrated that the cameras were synchronised to 1/100 of a second using two cables connected via a single operation relay switch. The same approach was also used in this study. The cameras were pre-calibrated at Loughborough University using a testfield calibration approach with the zoom

Figure 3. Survey staff positioned close to the water surface

lenses fixed to a nominal focal length setting of 24 mm. The determined radial distortion curve of one of the cameras is presented in Figure 4. The camera to object distance was approximately 8 m. An oblique image pair of the river surface was captured using the normal image configuration, whilst a second image pair was derived using a convergent configuration. The convergent angle between the camera axes was approximately 10 degrees and intersected the object plane at the same point. The combined imaging angles added up to approximately 30 degrees for both image pairs captured. The image pairs were processed using the Leica Photogrammetry Suite (LPS, Version 9.1) software. Photogrammetric control was provided by the target points along the river banks and interior orientation parameters were supplied by pre-calibration.
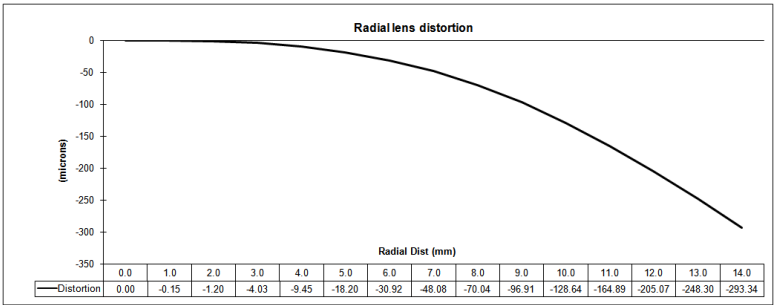

	0.0	1.0	2.0	3.0	4.0	5.0	6.0	7.0	8.0	9.0	10.0	11.0	12.0	13.0	14.0
Distortion	0.00	-0.15	-1.20	-4.03	-9.45	-18.20	-30.92	-48.08	-70.04	-96.91	-128.64	-164.89	-205.07	-248.30	-293.34

Figure 4. Radial distortion curve for one of the Nikon D80 cameras

Figure 5. Camera setup on the river at Loughborough

RESULTS AND DISCUSSION

Simulation

Research conducted in Wackrow and Chandler (2008) demonstrated that a mildly convergent image configuration minimises domes arising from an inaccurate lens model, but only vertical imagery had been tested. Similar results were expected using a mildly convergent image configuration in the oblique case but no explicit tests had been undertaken. A remaining question is why the convergent geometry reduces this particular systematic effect, which is best explained by Figure 6. In normal case configuration, the applied radial distortion correction for object point A in the image space is significantly different in the left and right image ($\Delta r_{a'} \neq \Delta r'_{a'}$). If an inaccurate lens model is used, rays of the left and right image intersect above the x-y object plane to A'. This effect is represented in the normal case for object points A' and B' in Figure 6 and causes the dome effect. However, the applied radial distortion correction for an object point is similar in the convergent configuration for the left and right image ($\Delta r_{a'} = \Delta r'_{a'}$). In this case the rays intersect in the X-Y object plane, even if an inaccurate lens model is present. Consequently, the dome effect is minimised. Figure 6 also demonstrates the introduction of a lateral displacement in the X-Y object plane. Unlike the dome effect, this systematic lateral displacement can be compensated through re-estimation of the exterior orientation by least squares.
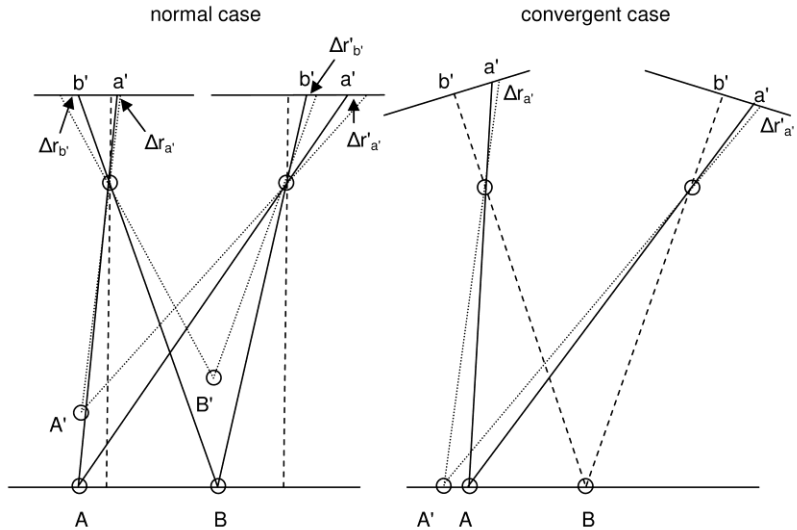
Figure 6. Effect of inaccurate radial distortion values

Two sets of exterior orientation describing a normal and convergent image configuration with the imaging angle set to 45 degrees were used in the simulation. The lens model was 20% inaccurate. It was judged that a variety of visualisations of the distortion surfaces, which included discrepancies in *X, Y, Z* was necessary to improve understanding. A Matlab routine was developed, which generates not only a surface representation but also computes distortion vectors for each point of the virtual test object. The individual distortion vectors demonstrate the direction of distortion of a surface at each point on the virtual test object. The derived surfaces and distortion vectors (Figures 7 and 8) represent an imaging angle of 45 degrees achieved using the normal configuration, whilst Figures 9 and 10 represent results achieved using the same imaging angle of 45 degrees but a convergent configuration. As expected, the mildly convergent image configuration almost eradicated the dome, even though an oblique convergent image pair was used. Various tests were conducted using a diversity of imaging angles and similar results, such as above, were obtained (Wackrow, 2008). These are not presented here for brevity.
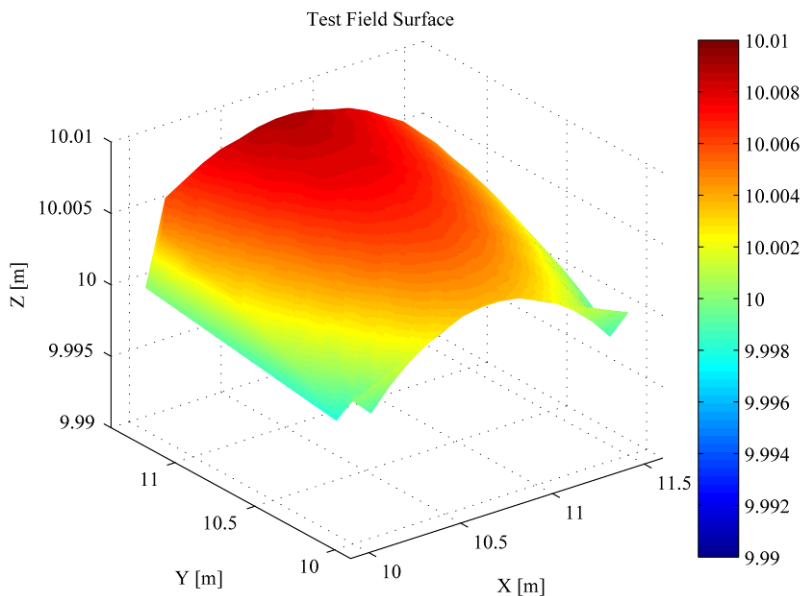
Test Field Surface

Figure 7. Virtual testfield surface oblique normal case (imaging angle 45 degrees)
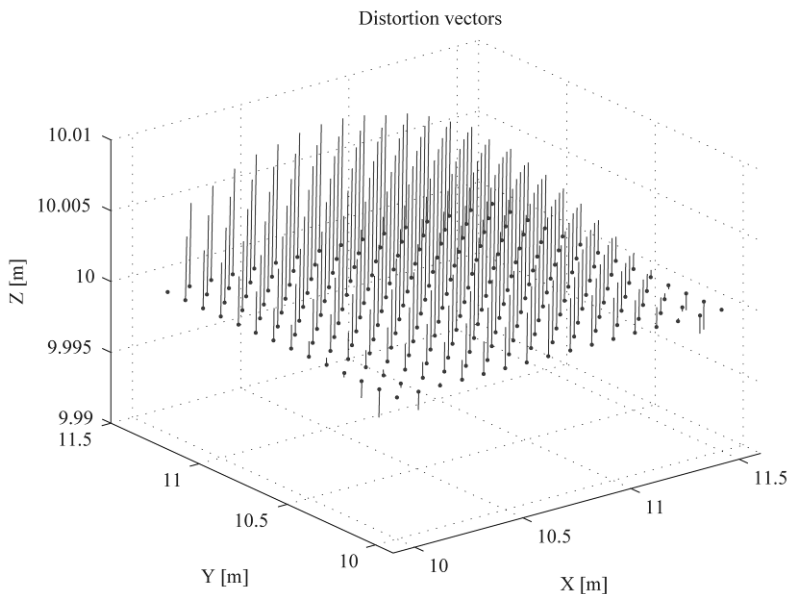
Distortion vectors

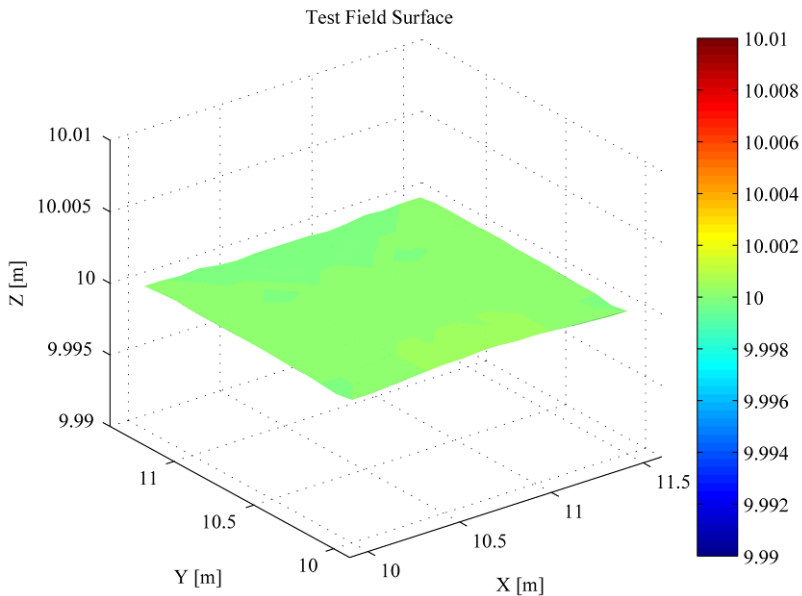Figure 8. Distortion vectors oblique normal case (imaging angle 45 degrees)

Figure 9. Virtual testfield surface oblique convergent case (imaging angle 45 degrees)
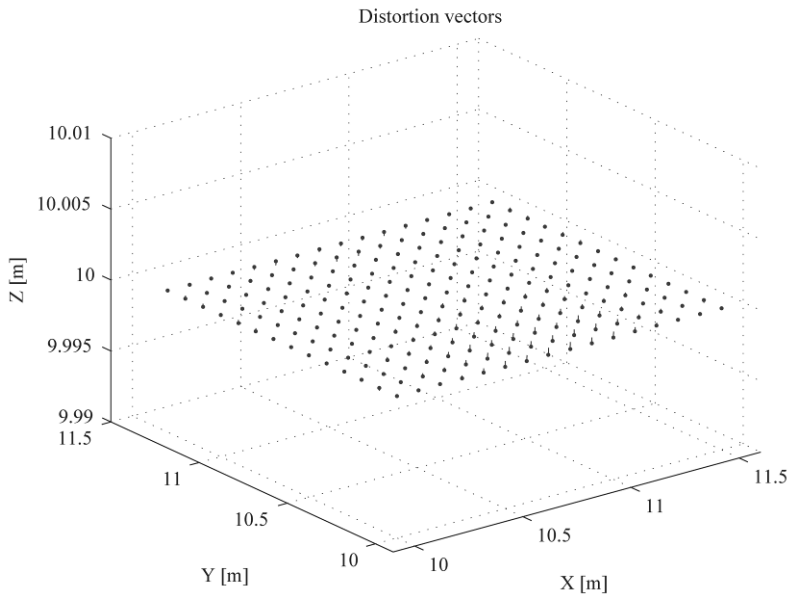

Figure 10. Distortion vectors oblique convergent case (imaging angle 45 degrees)

Laboratory testfield

Results of the simulation presented in the previous section demonstrated that an oblique convergent image configuration used for DEM generation minimises systematic errors caused by an inaccurate estimated lens model. To verify these results, a testfield of known geometry was used in a practical test to determine statistical values with sufficient reliability to quantify the optimum accuracy in the object space. An image pair representing the whole of the testfield and describing the normal oblique configuration was captured. The camera to object distance was approximately 2 m and an imaging angle of approximately 45 degrees was used. This image pair was processed in LPS using interior orientation parameters derived in a previous calibration session. However, the lens model was deliberately distorted by 20% for various reasons. Firstly, to be able to establish similar conditions used in the simulation; secondly, to emphasise the systematic effects caused by an inaccurate lens model, and finally to highlight the potential of the oblique convergent image configuration to minimise these systematic effects in derived DEM's.

Figure 11 represents the derived elevation differences (scaled to ± 5 mm) by comparing the "Truth DEM" with the automatically extracted DEM using the oblique normal configuration. A dome of similar shape identified in the simulation is clearly identifiable in the centre of the DEM of difference. Wooden blocks and adjacent areas indicate gross errors caused by shadowing effects. These would distort the accuracy statistics and were excluded prior to deriving mean error and standard deviation of error of the DEM of difference. A mean error of 3 mm and a standard deviation of ±6 mm were determined for the flat part of the testfield.
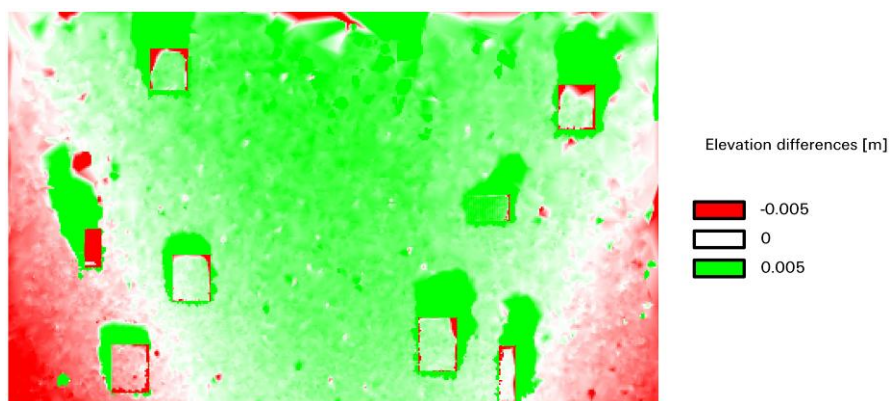

Elevation differences [m]

-0.005
0
0.005

Figure 11. Elevation differences oblique normal configuration

The procedure described for the normal configuration was similarly repeated using an oblique convergent image. The convergence angle used was approximately 10 degrees, whilst the imaging angle and the interior orientation parameters including the 20% disturbed lens model remained unchanged. LPS uses a hierarchical hybrid based technique to perform digital image matching which is a combination of area based and feature based image matching. Using a

convergent angle of approximately 10 degrees in this study identified no image matching problems but higher convergent angles could cause failures within matching, particularly using an area based image matching technique. Practical users should carefully consider this aspect. The derived DEM of difference (scaled to ± 5 mm) representing the oblique convergent configuration is illustrated in Figure 12. The dome identified in Figure 11 has been eradicated. A determined mean error of 0.9 mm and a standard deviation of ±5 mm also indicate that the systematic errors caused by the inaccurate lens model have been significantly reduced using the oblique convergent image configuration. The results determined in the practical test using a laboratory testfield confirm results achieved in the simulation process.
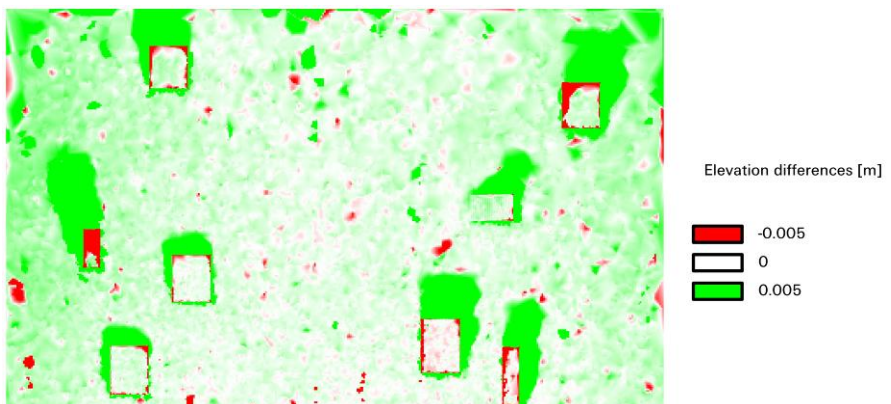

Figure 12. Elevation differences oblique convergent configuration

Measuring the dynamic water surface

The final practical test involved measuring the river surfaces, conducted in true field conditions. An adequate number of check points, not including those used to compute the restitution of the image pair, can provide independent data to assess the accuracy in the object space. These check point data were provided by the major staff graduations of the surveying staff (Figure 3). Residuals for the staff graduations in the X and Z plane, established using the normal image configuration are represented in Figure 13. A systematic pattern which is consistent with the presence of a dome can be clearly identified. This systematic effect is also indicated by a mean error of 2.2 mm, whilst random errors are represented by a standard deviation of ± 3.9 mm. Additionally, the lens model used in this case study has proven to be slightly inaccurate in the practical test conducted in Wackrow and Chandler (2008), so that the residual systematic errors identified can be attributed to this. Residuals for the staff graduations in the X and Z plane, determined using the convergent image configuration are represented in Figure 14. Comparison with Figure 13 clearly demonstrates that the systematic effects are reduced using the convergent image configuration, which is also summarised by a mean error of 0.7 mm (2.2 mm normal configuration). The random errors were also reduced, which is identified by the standard deviation of

± 2.1 mm (± 3.9 mm normal configuration). This result is significant as it implies that the mildly convergent image configuration has certainly reduced the residual systematic errors caused by an inaccurate lens model and verifies the findings of the simulation and laboratory test presented previously.

After an appropriate restitution of the oblique convergent stereo pair was established, a DEM representing the water surface could be extracted using the DEM generation capabilities of LPS. However, it was essential to provide a sufficient number of evenly distributed tie points representing the water surface of the river. Biodegradable foam packing chips were identified in Chandler et al (2008) as suitable seeding material and were also used in this practical test. An appropriate number of tie points could be generated using the automatic tie point generation tool of LPS, and a DEM with a resolution of 5 mm was extracted. These data were then transferred into a MATLAB routine to create a visualisation of the water surface (Figure 15). The position of the survey staff is clearly identifiable in this illustration. It is also notable that the physical structure of the dynamic water surface is well presented.
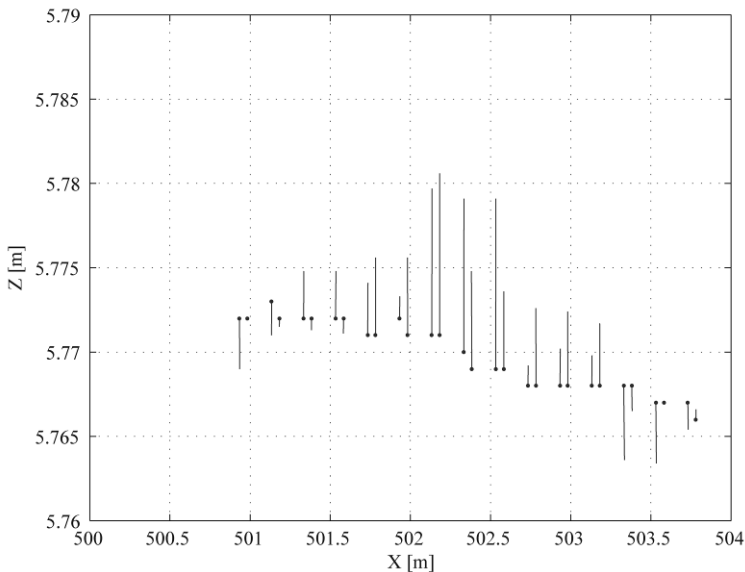

Figure 13. Distortion vectors of the survey staff graduations (normal configuration)
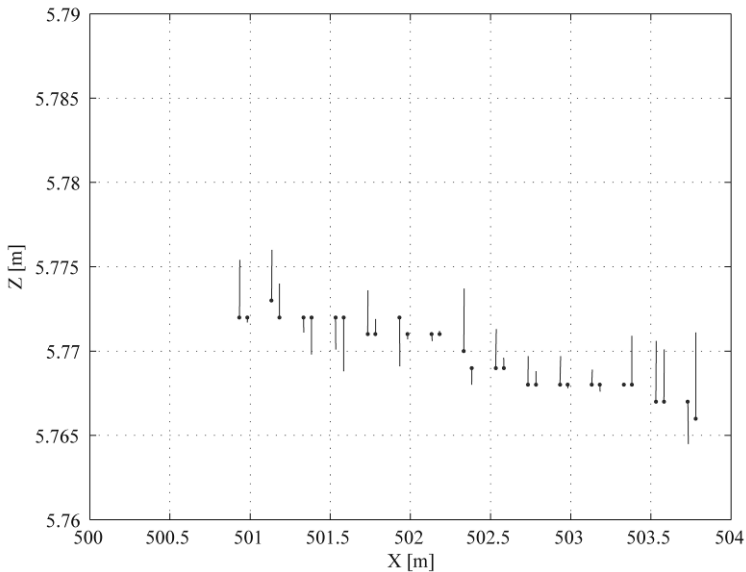
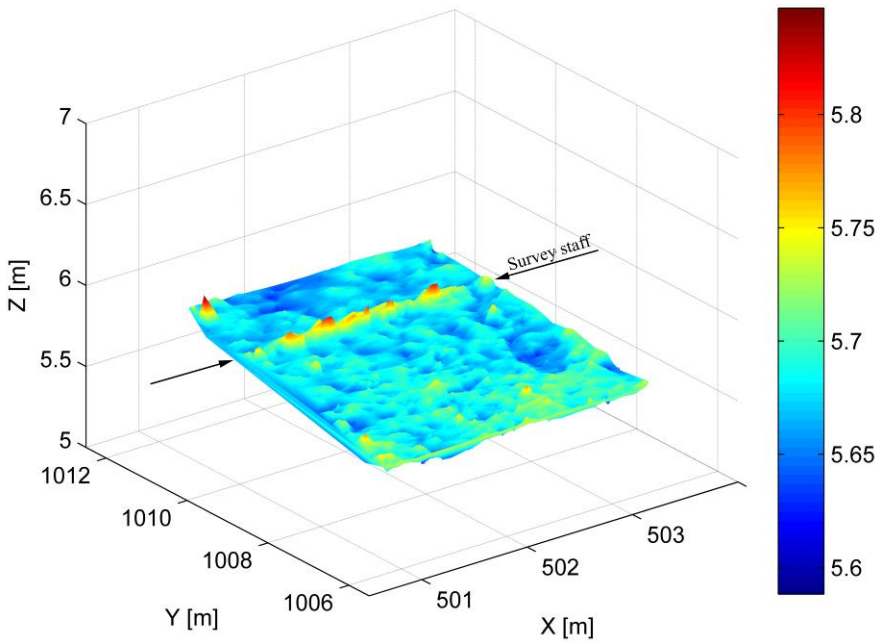Figure 14. Distortion vectors of the survey staff graduations (convergent configuration)

Figure 15. Loughborough river surface

CONCLUSION

The findings presented in this paper demonstrate that an oblique convergent image configuration reduces systematic errors in DEMs, which are caused by inaccurately estimated lens distortion parameters. This is significant because it perhaps identifies a new approach to increasing the accuracy of optical 3D measurement systems. In the past, the focus has been solely on camera calibration to minimise systematic effects in the object space. However, instead of concentrating solely on camera calibration, a new focus should perhaps be on image configuration. The results and findings presented demonstrate that a convergent image configuration for DEM extraction reduces the need for establishing a highly accurate lens model through conventional camera calibration methods. This also opens up new opportunities for the wider application of consumer grade digital cameras for spatial measurement.

ACKNOWLEDGEMENTS

REFERENCES

CHANDLER, J.H. AND CLARK, J.S. 1992. The archival photogrammetric technique: further applications and development. *Photogrammetric Record*, 14 (80): 241-247.

CHANDLER J.H., BUFFIN-BELANGER, T., RICE, S., REID, I. AND GRAHAM, D.J., 2003. The accuracy of a river bed moulding/casting system and the effectiveness of a low-cost digital camera for recording river bed fabric. *Photogrammetric Record*, 18 (103): 209-223.

CHANDLER, J.H., FRYER, J.G. AND JACK, A., 2005. Metric capabilities of low-cost digital cameras for close-range surface measurement. *Photogrammetric Record*, 20 (109): 12-26.

CHANDLER, J.H., WACKROW, R., SUN, X., SHIONO, K. AND RAMESHWARAN, P., 2008. Measuring a dynamic and flooding river surface by close range photogrammetry. *International Archives of Photogrammetry, Remote Sensing and Spatial Information Science*, 37 (Part B8): 211-216. (on CD-ROM).

COOPER, M.A.R. AND CROSS, P.A., 1988. Statistical concepts and their application in photogrammetry and surveying. *Photogrammetric Record*, 12 (71): 637-663.

FRASER, C.S., 1997. Digital camera self-calibration. *ISPRS Journal of Photogrammetry and Remote Sensing*, 52 (4): 149-159.

FRASER, C.S., 2006. Evolution of network orientation procedures. *International Archives of Photogrammetry, Remote Sensing and Spatial Information Science*, 36 (5), 114-120.

FRYER, J.G. AND MITCHELL, H.L., 1987. Radial distortion and close range stereophotogrammetry. *Australian Journal of Geodesy, Photogrammetry and Surveying*, 46 (47): 123-138.

FRYER, J.G., CHANDLER, J.H. AND COOPER, M.A.R. 1994. On the accuracy of heighting from aerial photographs and maps: implications to process modellers. *Earth Surface Processes and Landforms*, 19: 577-583.

GRANSHAW, S.I., 1980. Bundle adjustment methods in engineering photogrammetry. *Photogrammetric Record*, 10 (56): 181-207.

GRENNESS, M.J., OSBORN, J.E. AND TYAS, M.J., 2005. Stereo-photogrammetric mapping of tooth replicas incorporating texture. *Photogrammetric Record*, 20 (110): 147-161.

HOTHMER, J., 1958. Possibilities and limitations for elimination of distortion in aerial photographs. *Photogrammetric Record*, 2 (12): 426-445.

HOTHMER, J., 1959. Bundle Possibilities and limitations for elimination of distortion in aerial photographs (concluded). *Photogrammetric Record*, 3 (13): 60-78.

KARARA, H.M. AND ABDEK-AZIZ, Y.I., 1974. Accuracy aspects of non-metric imageries. *Photogrammetric Engineering*, 40 (9): 1107-1117.

LUHMANN, T., ROBSON, S., KYLE, S. AND HARLEY, I., 2006. Close Range Photogrammetry, Whittles, Caithness: 510 pages.

MAAS, H.-G., 1999. Ein Ansatz zur Selbstkalibrierung von Kameras mit stabiler innerer Orientierung. *Publikationen der Deutschen Gesellschaft für Photogrammetrie und Fernerkundung*, Band 7 (Eds. J. Albertz and S.W. Dech). Weinert, Berlin: 496 pages.

STOJIC, M., CHANDLER, J.H., ASHMORE, P. AND LUCE, J., 1998. The assessment of sediment transport rates by automated digital photogrammetry. *Photogrammetric Engineering and Remote Sensing*, 64 (5), 387-395.

REMONDINO, F. AND FRASER, C.S., 2006. Digital camera calibration methods: considerations and comparisons. *International Archives of Photogrammetry, Remote Sensing and Spatial Information Science*, 36 (5), 266-272.

REMONDINO, F. AND MENNA, F., 2008. Image-based surface measurement for close-range heritage documentation. *International Archives of Photogrammetry, Remote Sensing and Spatial Information Science*, 37 (Part B5): 199-206. (on CD-ROM).

REMONDINO, F., PETTI F.M., AVANZINI M. AND GIRARDI S. , 2010. 3D ichnology - recovering digital 3D models of dinosaur footprints. *Photogrammetric Record*, September 2010, in press.

ROBSON, S., ROVA, M., MORGAN, L., HEUMAN, J., HEATHCOTE, M., LEES, D., CANER, H. AND MILLS, C.G., 2008. Measurement of transparent plastic sculptures using photogrammetry, laser scanning and tough probing for conservation purposes. *International Archives of Photogrammetry, Remote Sensing and Spatial Information Science*, 37 (Part B5): 207-212. (on CD-ROM).

WACKROW, R., CHANDLER, J.H. AND BRYAN, P., 2007. Geometric consistency and stability of consumer-grade digital cameras for accurate spatial measurement. *Photogrammetric Record*, 22 (118), 121-134.

WACKROW, R, 2008. Spatial measurement with consumer grade digital cameras. *PhD Thesis*, Loughborough Repository: https://dspace.lboro.ac.uk/dspace-jspui/handle/2134/3827: 196 pages.

WACKROW, R. AND CHANDLER, J.H., 2008. A convergent image configuration for DEM extraction that minimises the systematic effects caused by an inaccurate lens model. *Photogrammetric Record*, 23 (121), 6-18.

WACKROW, R., CHANDLER, J.H. AND GARDNER, T., 2008. Minimising systematic errors in DEMs caused by an inaccurate lens model. *International Archives of Photogrammetry, Remote Sensing and Spatial Information Science*, 37 (Part B5): 1-6. (on CD-ROM).

Zusammenfassung

Digitale Amateurkameras werden zunehmend benutzt, besonders wenn präzise räumliche Daten erfasst werden können. Kürzlich durchgeführte Forschungen an der Loughborough University identifizierten Oberflächen mit systematischen Fehlern oder "Kuppeln", sichtbar in digitalen Höhenmodellen (DEMs). Diese systematischen Effekte sind häufig mit solchen Kameras verbunden und und werden verursacht durch ungenau berechnete Verzeichnungsparameter. Eine Methode, welche eine geringe konvergente lotrechte Kamerakonfiguration verwendet und diese systematischen Fehler der Oberflächen minimiert, wurde entwickelt. Diese Methode wurde durch Simulationen und eine Reihe praktischer Untersuchungen getestet. Dieser Artikel untersucht das Potential der konvergenten Kamerakonfiguration, die Oberflächenfehler zu minimieren, selbst wenn die geometrisch komplexere Schrägansicht benutzt wird. Zunächts wurden simulierte Daten verwendet, um zu demonstrieren, das eine schräge konvergente Kamerakonfiguration unter Benutzung verschiedener Blickwinkel, die verbleibenden systematischen Fehler der Oberflächen minimiert. Zusätzlich wurden praktische Tests durchgeführt, wobei ein laboratorisches Testfeld

verwendet wurde, um die Ergebnisse der Simulation zu verifizieren. Die Notwendigkeit, ein System zu entwicklen, welches die topographische Oberfläche eines fließenden Flusses messen kann, bot die Gelegenheit, die Resultate der Simulation und des Labortests mit realen Daten zu verifizieren. Die Ergebnisse der Simulation, des Labortests und des praktischen Tests sind in diesem Artikel beschrieben und demonstrieren, das eine schräge konvergente Kamerakonfiguration die systematischen Fehler der Oberflächen, eleminiert, welche verursacht wurden durch ungenau berechnete Verzeichnugsparameter.